This is a preprint, the final version is subject to change, of the American Mineralogist (MSA)
Cite as Authors (Year) Title. American Mineralogist, in press.
DOI: https://doi.org/10.2138/am-2018-6386

Geochemical constraints on residual metal and sulfide in the sources of lunar mare basalts

James M.D. Day

Scripps Institution of Oceanography, University of California San Diego, La Jolla, CA 92093-0244, USA

Submission to *American Mineralogist, manuscript 6368 REVISION 2*

'Planetary Processes as Revealed by Sulfides and Chalcophile Elements'

Abstract: 336

Main Text: 3392

References: 60

Figures: 7

Tables: 1

This is a preprint, the final version is subject to change, of the American Mineralogist (MSA)
Cite as Authors (Year) Title. American Mineralogist, in press.
DOI: https://doi.org/10.2138/am-2018-6386

Abstract

Low oxygen fugacity (fO_2) in the lunar interior (one log unit below the iron-wüstite buffer [IW-1]) offers the possibility that stable Fe-metal and sulfide phases exist as restites within lunar mare basalt source regions. Metal and sulfide phases have high metal-melt and sulfide-melt partition coefficients for chalcophile, siderophile (>100), and highly siderophile elements (>>100,000 - HSE: Os, Ir, Ru, Rh, Pt, Pd, Re, Au). If these phases are residual after mare basalt extraction, they would be expected to retain significant quantities of these elements, likely generating non-chondritic HSE inter-element ratios, including Re/Os in the silicate magma. If such phases were present, the estimated HSE abundances of the bulk silicate Moon (BSM) would be proportionally higher than current estimates (0.00023 ±2 × CI chondrite), and perhaps closer to the bulk silicate Earth (BSE) estimate (0.009 ±2 × CI chondrite). Here I show that relationships between elements of similar incompatibility but with siderophile (W), chalcophile (Cu) and lithophile tendencies (Th, U, Yb) do not deviate from expected trends generated by magmatic differentiation during cooling and crystallization of mare basalts. These results, combined with chondrite-relative HSE abundances and near-chondritic measured $^{187}Os/^{188}Os$ compositions of primitive high-MgO mare basalts, imply that lunar mantle melts were generated from residual metal- and sulfide-free sources, or experienced complete exhaustion of metal and sulfides during partial melt extraction. Evidence for the loss of moderately volatile elements during lunar formation and early differentiation indicates that the BSM is >4 to 10 times more depleted in S than BSE. Because of an S-depleted BSM, mare basalt melts are unlikely to have reached S saturation, even if sulfide concentration at sulfide saturation (SCSS) was lowered relative to terrestrial values due to low lunar fO_2. In the absence of residual sulfide or metal, resultant partial melt models indicate that a lunar mantle source with 25 to 75 μg g^{-1} S and high

This is a preprint, the final version is subject to change, of the American Mineralogist (MSA)
Cite as Authors (Year) Title. American Mineralogist, in press.
DOI: https://doi.org/10.2138/am-2018-6386

sulfide-melt partition coefficients can account for the chondritic relative abundances of the HSE in mare basalts from a BSM that experienced <0.02% by mass of late accretion.

Keywords: Moon; siderophile elements; sulfide; metal; saturation; partial melting

Introduction

The bulk composition of the Moon places fundamental constraints on its formation (e.g., Taylor et al., 2006; Warren & Taylor, 2014). No lunar mantle samples are available for study, making estimates of the bulk silicate Moon (BSM) feasible only by extrapolation of the composition of lunar surface rocks, including ferroan anorthosites and mare basalts. The concentrations of the highly siderophile elements (HSE: Os, Ir, Ru, Rh, Pt, Pd, Re, Au) for the BSM have been estimated by measurements of crustally uncontaminated mare basalts, and regression of these data to an assumed mare basalt source (aka, the lunar mantle) using MgO-regression methods (Warren et al., 1989; Day et al., 2007; Day & Walker, 2015). Since mare basalts come from partial melting of the lunar interior, and the great majority of the HSE should be in their olivine + pyroxene ± ilmenite bearing sources relative to ultra-low HSE abundance crustal rocks (Day et al., 2010), then the BSM can be estimated directly to have chondrite-relative HSE abundances ~0.00023 ±2 × CI chondrites, with present-day $^{187}Os/^{188}Os$ of ~0.1293 (Day et al., 2007; 2016). The MgO-regression method has also been used to obtain the bulk silicate Earth (BSE) HSE composition from terrestrial lavas (e.g., Day et al., 2007; 2016), resulting in good agreement with the chondrite-relative BSE HSE abundances determined from peridotites (0.009 ±2 × CI chondrite, $^{187}Os/^{188}Os$ = 0.1296 ±8; Meisel et al., 2001; Becker et al., 2006; Day et al., 2017) (**Figure 1**).

This is a preprint, the final version is subject to change, of the American Mineralogist (MSA)
Cite as Authors (Year) Title. American Mineralogist, in press.
DOI: https://doi.org/10.2138/am-2018-6386

64

65 The BSM HSE estimate is more than 30 times lower than the BSE HSE estimate, a
66 depletion that has been attributed to a reduced contribution from late accretion materials to the
67 Moon relative to Earth (Walker et al., 2004; Day et al., 2007; Day & Walker, 2015). In this
68 model, draw-down of the HSE during the formation of the Moon in a giant impact event, and/or
69 during the formation of a small lunar core (e.g., Weber et al., 2011) led to nearly-quantitative
70 depletion of the HSE in the BSM, followed by limited late accretion of broadly chondritic
71 material to the Moon (~0.02 wt.%, or ~1.7×10^{19} kg) relative to Earth (~0.5 wt.%, or ~2×10^{22}
72 kg). This observation has been widely used as a constraint for dynamical models of planetary
73 accretion (e.g., Bottke et al., 2010; Schlichting et al., 2012; Jacobsen et al., 2014) and led to the
74 recent interpretation of W isotopic differences between Earth and the Moon as representing
75 disproportionate late accretion (Touboul et al., 2015; Kruijer et al., 2015).

76

77 An underlying concern when using mare basalts to determine the BSM HSE composition
78 is that regression methods, similar to those used to determine the BSE HSE composition using
79 terrestrial lavas, may not be effective due to substantially different oxygen (fO_2) and sulfur (fS_2)
80 fugacities for the two planetary bodies. It has been constrained that the Moon's mantle has a low
81 fO_2, at around one log unit below the iron-wüstite (IW) buffer (e.g., Sato et al., 1973; Wadhwa,
82 2008), whereas the Earth's mantle has greater than four orders of magnitude higher oxygen
83 activity, at the fayalite-magnetite-quartz (FMQ) buffer (e.g., Sato, 1978; Haggerty, 1978; Frost
84 and McCammon, 2008). It is therefore possible that metal is more stable and residual within
85 lunar mare basalt regions after partial melting than in Earth's mantle. Equally, low fO_2, might
86 lead to decreased sulfide concentration at sulfide saturation (SCSS) in mare basalts (Brenan et

This is a preprint, the final version is subject to change, of the American Mineralogist (MSA)
Cite as Authors (Year) Title. American Mineralogist, in press.
DOI: https://doi.org/10.2138/am-2018-6386

al., 2016), and thus favor the survival of residual sulfides during melting. The term SCSS represents the maximum amount of sulfur a silicate melt can dissolve and provides an upper boundary to S concentrations found in melts at reduced fO_2 conditions. Here I examine the possible role of residual metal or sulfide in the source during partial melting of mare basalts, focusing first on constraints placed on these processes by the HSE abundances and $^{187}Os/^{188}Os$ of mare basalts.

Constraints from the HSE and $^{187}Os/^{188}Os$ ratios of mare basalts

Mare basalts are ~3 to 3.9 Ga magmatically-derived rocks that formed by partial-melting of source regions within the Moon with mineralogy dominated by olivine + pyroxene ± ilmenite (e.g., Snyder et al., 1992). Mare basalt mantle sources are considered to have formed from crystallization of a lunar magma ocean resulting in initial mineralogical stratification followed by later mixing (e.g., Warren & Taylor, 2014). Two main types of mare basalts have been identified: low Ti variants (<5 wt.% TiO_2) that are considered to make up most of the mare basalts exposed at the lunar surface (Giguere et al., 2000) and that were primarily sampled at the Apollo 12 and 15 landing sites, and as mare basalt meteorites; and high Ti mare basalts (>6 wt.% TiO_2) that were primarily sampled at the Apollo 11 and 17 landing sites (Neal & Taylor, 1992). Despite originating from mineralogically variable sources, the most primitive and crustally uncontaminated high-MgO mare basalts from the Apollo 12 (samples 12004, 12040), 15 (samples 15016, 15555) and 17 sites (sample 74255) all have chondrite-relative abundances of the HSE and measured $^{187}Os/^{188}Os$ within the range of chondrites (0.1265 to 0.1345) (Day et al., 2007; Day & Walker, 2015). The $^{187}Os/^{188}Os$ ratio of mare basalts is a particularly powerful tracer of composition because the ancient crystallization ages of these rocks (3 to 3.9 Ga) only

This is a preprint, the final version is subject to change, of the American Mineralogist (MSA)
Cite as Authors (Year) Title. American Mineralogist, in press.
DOI: https://doi.org/10.2138/am-2018-6386

permit small deviations from a chondritic Re/Os ratio to obtain nearly chondritic $^{187}Os/^{188}Os$ measured today.

A histogram plot of measured mare basalt $^{187}Os/^{188}Os$ compositions illustrates that many of the samples have $^{187}Os/^{188}Os$ ratios that cluster around the range of chondrites, and within the BSE composition, with a tail to more radiogenic ratios (**Figure 2**). The radiogenic $^{187}Os/^{188}Os$ ratios are found in low-MgO samples and reflect increasing Re/Os during magmatic differentiation (Day & Walker, 2015). The HSE abundances that are in broadly chondritic proportions, and a Re/Os ratio within a few percent of the chondritic ratio are therefore key constraints on any successful partial melting model for generating primitive high-MgO mare basalts. Any fractionation of Re/Os away from the chondritic composition during metal-melt or sulfide-melt partitioning, for example, would not be permitted by the available mare basalt data.

Metal in mare basalt source regions

The low fO_2 of the Moon leads to the possibility that residual metal may have been present after partial melting to form mare basalts. Residual metal in the source would lead to near-quantitative retention of the HSE and could account for the low HSE abundance of mare basalts, if the chondritic proportions of the HSE can be reproduced by this process. Evidence for metal formation at low fO_2 during late-stage (>90% crystallization) magmatic differentiation is obtained from mare basalts themselves, which can contain ≤0.1 modal% FeNi-metal (e.g., Reid et al., 1970; Day et al., 2006). Formation of metal grains within mare basalts, however, does not equate to the presence of metal in mare basalt mantle sources. Reduction of Fe^{2+} to Fe^0 by eruptive degassing of S or C, or by reactions with Ti^{3+} or Cr^{2+} have all been considered as likely

This is a preprint, the final version is subject to change, of the American Mineralogist (MSA)
Cite as Authors (Year) Title. American Mineralogist, in press.
DOI: https://doi.org/10.2138/am-2018-6386

mechanisms for the presence of metal grains in mare basalts (e.g., Sato et al., 1976; Brett, 1976; Schreiber et al., 1982). Reduction of Fe by H is also possible for lunar mare basalt melts, in the reaction $FeO^{(+)} + H_2 \rightarrow Fe^{(+)} + H_2O$.

Previously, Day & Walker (2015) showed that W, U and Th are not strongly fractionated in Apollo 12 mare basalts, indicating that no residual metal existed in the sources of these mare basalts after their partial melt extraction. The choice of investigating W, U and Th is that these elements behave similarly during partial melting and fractional crystallization, but that W is a moderately siderophile element and U and Th are strongly incompatible lithophile trace elements. Any residual metal in the source after mare basalt partial melt extraction should lead to retention of W, but effective removal of Th and U. On the other hand, a lack of residual metal would lead all three elements to behave as highly incompatible lithophile trace elements.

To further evaluate this possibility for known mare basalt sources, W, U and Th data are reported for the Apollo 12 mare basalts presented in Day & Walker (2015), and for four mare basalt meteorites (MIL 05035, LAP 02205, NWA 4734 and Dho 287), which, except for NWA 4734 and Dho 287, have previously been measured for HSE abundances and Os isotopes (Day et al., 2007; Day & Walker, 2015) (for methods and data, see **Table 1**). In a plot of W versus U (**Figure 3**), residual metal in the source after mare basalt melt extraction would be expected to lead to very low W abundances for a given U content. As with the Apollo 12 mare basalts, the mare basalt meteorites fall along a linear correlation for W and U, and all samples have similar U/Th (0.243 ±0.028). The U/Th ratio constrains the relative proportions of these elements to be approximately the same as those of chondrites (0.283; Anders & Grevesse, 1989), Earth (0.276;

This is a preprint, the final version is subject to change, of the American Mineralogist (MSA)
Cite as Authors (Year) Title. American Mineralogist, in press.
DOI: https://doi.org/10.2138/am-2018-6386

Taylor & McLennan, 1985), and to the lunar surface (0.269 ±0.007; Yamashita et al., 2010). These results imply no significant modification of W/U ratios and indicate that metal is not a residual phase in the mantle sources of mare basalts. Published data for W and U contents are also available for the Apollo 11, 12, 15 and 17 mare basalts and, despite considerable scatter relative to the newly presented data, have high W for a given U content implying lack of residual metal during melt extraction.

Correlations of W versus U or Th, which involves equally incompatible trace elements, argue strongly for either residual metal-free sources, or complete exhaustion of metal during mare basalt partial melting. A collateral consequence of residual metal in the source of mare basalts would also be to strongly fractionate the HSE in partial melts due to the variable but high metal-silicate partition coefficients for the different HSE (e.g., Mann et al., 2012). Strong fractionations of the HSE are not observed in the primitive high-MgO mare basalts, and HSE patterns of low-MgO basalts can be entirely accounted for by near-surface crystal-liquid fractionation (Day & Walker, 2015).

Sulfur content of mare basalt source regions

In the absence of evidence for residual metal in the source of mare basalts, it is possible that residual sulfide can be retained in source regions during the genesis of mare basalts, due to extremely low fO_2. For the purposes of understanding mare basalt petrogenesis, there are two key questions that need to be addressed. First, how much S is likely to be in mare basalt sources and, second, how much S can be incorporated into the parental silicate magma without S saturation. Sulfur is a chalcophile and volatile element (50% condensation temperature [TC_{50}] = 664K;

This is a preprint, the final version is subject to change, of the American Mineralogist (MSA)
Cite as Authors (Year) Title. American Mineralogist, in press.
DOI: https://doi.org/10.2138/am-2018-6386

179 Lodders, 2003) and, along with some moderately volatile elements, including Zn and K (TC_{50} of
180 726 and 1006K, respectively), has been shown to be depleted in the Moon, relative to Earth, due
181 to volatile depletion (e.g., Paniello et al., 2012; Day & Moynier, 2014; Wing & Farquhar, 2015;
182 Wang & Jacobsen, 2016). Based on current estimates, this depletion is between three
183 (Bombardieri et al., 2005) and ten times greater in the BSM, relative to the BSE (**Figure 4**). This
184 leads to estimates of S in the BSM, or in the sources of mare basalts of between 75 and 25 μg g^{-1},
185 using a BSE S content of 250 μg g^{-1} (McDonough & Sun, 1995). These estimates are similar to
186 the inferred heterogeneous abundances of sulfur in the source regions of Apollo 11 (35-120 μg g^{-1}), 12 (27-92 μg g^{-1}), 15 (10-23 μg g^{-1}) and 17 (25-62 μg g^{-1}) mare basalts from recent
188 experimental constraints (Ding et al., 2018).
189
190 Regarding the second question of S-saturation of parental magmas, this is dependent on
191 the major-element composition of the magma, the composition of the immiscible sulfide, and the
192 temperature and pressure (e.g., O'Neill & Marvogenes, 2002; Holzheid & Grove, 2002).
193 Mavrogenes & O'Neill (1999) showed that sulfur content at sulfide saturation (SCSS) is
194 relatively independent of fS_2 and fO_2, except if the melt composition changes in FeO content.
195 The amount of FeO can vary dramatically in mare basalts as a function of source and parental
196 magma differentiation. SCSS is also dependent on the nature of the immiscible sulfide, which at
197 low fO_2 will have Fe/S >1, causing SCSS to fall. FeO content is therefore a dominant control on
198 SCSS. An important facet of these observations is that if magmas do not become S saturated
199 during differentiation then primitive parental melts were most likely not S-saturated (i.e., there
200 was no residual sulfide).
201

This is a preprint, the final version is subject to change, of the American Mineralogist (MSA)
Cite as Authors (Year) Title. American Mineralogist, in press.
DOI: https://doi.org/10.2138/am-2018-6386

To empirically examine whether sulfide saturation was reached in lunar melts, FeO and S contents of bulk rock mare basalts and of melt inclusions are shown in **Figure 5**, along with S-saturation curves established from several studies. Degassing of S during eruption would drive preserved S contents down in whole-rock mare basalts, but not in melt inclusions. In the bulk rocks, and the majority of melt inclusions with FeO >15 wt.%, none of the low-Ti (Apollo 12, Apollo 15) or high-Ti (Apollo 17) melts would be S-saturated relative to their respective saturation curves, and the likelihood of residual S in the source would be low, consistent with recent experimental evidence for S exhaustion during mare basalt partial melting (Ding et al., 2018). It should be noted that melt inclusions with <~15 wt.% FeO have likely experienced significant side-wall crystallization or equilibration with their host crystals, driving their compositions to the left in **Figure 5**. Collectively, these lines of evidence imply that primitive melts parental to mare basalts were likely undersaturated in sulfur.

Recently, Brenan et al. (2016) have reported - in abstract form - evidence that SCSS falls rapidly as fO_2 approaches metal saturation, resulting in an S-saturated source. So long as metal saturation is not reached, then in this scenario, even the melt inclusions with between 15 to 25 wt.% FeO in **Figure 5** would be close to the S-saturation curve, which would likely be below the corrected melt inclusion S-saturation trend of Bombardieri et al. (2005) that considers the effects of degassing of sulfur. Based on their experimental results, Brenan et al. (2016) have suggested that sulfides would remain in the residue during partial melting, retaining the HSE. Following this scenario, they postulate that the BSM HSE abundance may only be ~4 times less than the BSE HSE contents.

This is a preprint, the final version is subject to change, of the American Mineralogist (MSA)
Cite as Authors (Year) Title. American Mineralogist, in press.
DOI: https://doi.org/10.2138/am-2018-6386

225 **Melting processes during the formation of mare basalts**

226 To evaluate the role of sulfides during lunar mantle partial melting, melting models are
227 explored to reproduce melting effects on the HSE. Partitioning of the HSE between sulfide melt
228 and silicate melt has been shown to have *D* values of 10^3 to 10^6 in both experiments and studies
229 of natural samples (e.g., Mungall & Brenan, 2014). In a recent assessment of sulfide melt-silicate
230 melt partitioning experiments Mungall & Brenan (2014) showed that values of *D* can be as high
231 as 2-3 × 10^6 for Ir and Pt. Even though these experiments were conducted at ΔFMQ -0.7 to -2.4
232 (i.e., more oxidizing than lunar conditions, at ~ΔIW +1.6 to +3), they offer the best estimates of
233 sulfide-melt silicate-melt partitioning and the constructed models therefore explore *D* values
234 from low (10,000) to high (1,000,000; **Figure 6**). Three melting models are investigated: (1)
235 terrestrial conditions with ~250 μg g^{-1} S and BSE HSE abundances from Becker et al. (2006) and
236 Day et al. (2017). This model indicates S exhaustion at ~23% partial melting (*F*); (2) a lunar
237 mantle with BSM HSE concentrations reported in Day et al. (2007; 2016) and source S contents
238 at the high end of the S estimate of the BSM (75 μg g^{-1}); (3) a lunar mantle with HSE
239 abundances ~4 times lower than in BSE, but with a BSM S content of 75 μg g^{-1}. The last two
240 models require S exhaustion at ~8% partial melting using estimates of SCSS from Bombarderi et
241 al. (2005) and 10-14% partial melting for lower SCSS, as illustrated in **Figure 6**.
242
243 The models highlight several important issues for mare basalt petrogenesis. In the first
244 instance, without complete S exhaustion in the source, and with extreme sulfide-melt partition
245 coefficients, the likelihood for HSE inter-element fractionation is significant. Variable sulfide
246 liquid-silicate liquid D values can lead to extreme sulfide-melt partition coefficients, with Pt/Os,
247 Pd/Os and - in particular - Re/Os ratios that can become extremely fractionated (e.g., **Figure 6b**).

This is a preprint, the final version is subject to change, of the American Mineralogist (MSA)
Cite as Authors (Year) Title. American Mineralogist, in press.
DOI: https://doi.org/10.2138/am-2018-6386

248 This effect is apparent from the variable HSE partitioning observed by Mungall & Brenan (2014)
249 for Pt (D = ~4400 to 1,560,000), Ir (D = 48,000 to 1,900,000) and Pd (D = 67,000 to 536,000). A
250 firm constraint on viable models for partial melting of mare basalt sources, therefore, is that the
251 melting results in chondrite-relative abundances of the HSE and long-term Re/Os within a few
252 percent of chondrites to satisfy primitive mare basalt compositions. Second, the melting intervals
253 required to explain mare basalt compositions from a source with low SCSS and HSE contents
254 only ~4 times lower than in the BSE are highly restricted, with very steep melting curves
255 (**Figure 6**). In contrast, a BSM with low HSE contents (e.g., Day et al., 2007; 2016) and low
256 sulfide-melt partition coefficients can readily generate the HSE compositions of primitive mare
257 basalts, within the range of acceptable partial melting (5 to 11%). The models are strongly driven
258 by the S contents in the mantle sources of mare basalts and, with high D values, imply generation
259 of mare basalts from source regions that did not retain residual sulfide. This result is consistent
260 with the recent experimental results of Steenstra et al. (2018) indicating that mare basalt and
261 pyroclastic glass bead source regions were not sulfide saturated.
262
263 **Sulfide in mare basalt source regions**
264 As with metal retention in the mantle, a further constraint on any residual sulfide phases
265 in mare basalt source regions can be placed by study of elements with similar incompatibility but
266 differing lithophile or siderophile tendencies. For this purpose, Cu and Yb can be used, as both
267 elements have similar incompatibility during magmatic differentiation. Copper is a chalcophile
268 and moderately volatile element that is estimated to be at lower abundance in the BSM (~3.3 μg
269 g^{-1}; O'Neill, 1991) relative to BSE (~27 μg g^{-1}; McDonough & Sun, 1995), whereas Yb is a
270 refractory lithophile element. During magmatic differentiation on the Moon, Yb is incompatible,

This is a preprint, the final version is subject to change, of the American Mineralogist (MSA)
Cite as Authors (Year) Title. American Mineralogist, in press.
DOI: https://doi.org/10.2138/am-2018-6386

forming a negative correlation with MgO (**Figure 7a**). The positive correlation between Yb and Cu indicates that Cu variations in mare basalts are a function of crystal-liquid fractionation, with the most primitive Apollo 12 mare basalts having ~6 to 8 μg g^{-1} Cu (**Figure 7b**). The correlation between Cu and Yb argues strongly for undersaturation of S during partial melting, consistent with evidence from Apollo 12 olivine melt inclusions (Bombardieri et al., 2005). Collectively, these results indicate that mare basalt melts were not sulfide saturated.

Conclusions and Implications

Current estimates of the siderophile and HSE contents of the lunar mantle assume that the source regions of mare basalts are free of residual metal and sulfide phases. Siderophile and HSE contents would inevitably be underestimated in the lunar mantle if this assumption was invalid. Currently, there is no strong geochemical evidence for residual metal or sulfide saturation after mare basalt partial melt extraction. Low S contents (25-75 μg g^{-1}) are likely in the bulk silicate Moon, considering the evidence for loss of moderately volatile elements including Cl, S, K and Zn during formation and differentiation of the Moon, further limiting the likelihood for residual sulfide in mare basalt sources. Potential draw-down of S into a lunar core has not been accounted for but would lead to the inevitable conclusion that the S contents of the BSM are >4 times lower than in the BSE. Melting models for the HSE indicate that high sulfide-melt partition coefficients and an HSE-poor bulk silicate Moon (BSM) can account for the chondrite-relative abundances of the HSE and near-chondritic measured $^{187}Os/^{188}Os$ in primitive mare basalts from the Apollo 12, 15 and 17 sites. The very low (0.00023 ±2 × CI chondrite) and chondritic relative composition of the BSM HSE remains a robust constraint on the quantity of materials added during late accretion that are present in mare basalt sources. In turn, this suggests that the Moon experienced

This is a preprint, the final version is subject to change, of the American Mineralogist (MSA)
Cite as Authors (Year) Title. American Mineralogist, in press.
DOI: https://doi.org/10.2138/am-2018-6386

294 disproportionately low late accretion compared to the Earth and that S and other volatile
295 elements were not added in significant quantity by late accretion to the Moon.
296
297 **Acknowledgements**
298 This work is dedicated to a mentor, friend and 'lunatic', Lawrence (Larry) A. Taylor, whose
299 enthusiasm for lunar science was truly infectious. I thank Clive Neal for providing a copy of his
300 mare basalt database and Rich Walker, Bill McDonough and James Brenan for thought-
301 provoking discussions. Reviews from Laurie Reisberg, Ying Xia, Graham Pearson, an
302 anonymous reviewer and the associate editor, Kate Kiseeva, are gratefully acknowledged.
303 Financial support to complete this work came from the NASA Solar System Workings program
304 (NNX16AR95G).
305
306 **References**

307 Anders E, and Grevesse N (1989) Abundances of the elements: meteoritic and solar. Geochimica
308 et Cosmochimica Acta 53, 197–214
309 Becker H, Horan MF, Walker RJ, Gao S, Lorand J-P, and Rudnick RL (2006) Highly siderophile
310 element composition of the Earth's primitive upper mantle: Constraints from new data on
311 peridotite massifs and xenoliths. Geochimica et Cosmochimica Acta 70, 4528-4550
312 Bombarderi DJ, Norman MD, Kamentsky VS, and Danyushevsky LV (2005) Major element and
313 primary sulphur concentrations in Apollo 12 mare basalts: the view from melt inclusions.
314 Meteoritics and Planetary Science 40, 659-671
315 Bottke WF, Walker RJ, Day JMD, Nesvorny D, and Elkins-Tanton L (2010) Stochastic late
316 accretion to Earth, the Moon, and Mars. Science 330, 1527-1530

317 Brenan JM, Mungall JE, Homolova V, and Luo D (2016) A sulfide-saturated lunar mantle? 4th
318 Highly Siderophile Element Workshop, p 35
319 Brett R (1976) Reduction of mare basalts due to sulfur loss. Geochimica et Cosmochimica Acta
320 40, 997-1004
321 Chen Y, Zhang Y, Liu Y, Guan Y, Eiler J, and Stolper EM (2015) Water, fluorine, and sulfur
322 concentrations in the lunar mantle. Earth and Planetary Science Letters 427, 37-46
323 Dankwerth PA, Hess PC, and Rutherford MJ (1979) The solubility of sulfur in high-TiO_2 mare
324 basalts. Proc. Lunar Planet. Sci. Conf. 10th, 517-530
325 Day JMD (2013) Hotspot volcanism and highly siderophile elements. Chemical Geology, 341,
326 50-74
327 Day JMD, and Moynier F (2014) Evaporative fractionation of volatile stable isotopes and their
328 bearing on the origin of the Moon. Philosophical Transactions of the Royal Society A
329 20130259. http://dx.doi.org/10.1098/rsta.2013.0259
330 Day JMD, and Walker RJ (2015) Highly siderophile element depletion in the Moon. Earth and
331 Planetary Science Letters, 423, 114-124
332 Day JMD, Taylor LA, Floss C, Patchen AD, Schnare DW, and Pearson DG (2006) Comparative
333 petrology, geochemistry and petrogenesis of evolved, low-Ti lunar mare basalt meteorites
334 from the La Paz icefield, Antarctica. Geochimica et Cosmochimica Acta 70, 1581-1600
335 Day JMD, Pearson DG, and Taylor LA (2007) Highly siderophile element constraints on
336 accretion and differentiation of the Earth-Moon system. Science 315, 217-219
337 Day JMD, Walker RJ, James OB, and Puchtel IS (2010) Osmium isotope and highly siderophile
338 element systematics of the lunar crust. Earth and Planetary Science Letters 289, 595-605

339 Day JMD, Brandon AD, and Walker RJ (2016) Highly Siderophile Elements in Earth, Mars, the
340 Moon, and Asteroids. Reviews in Mineralogy and Geochemistry 81, 161-238
341 Day JMD, Walker RJ, and Warren JM (2017) ^{186}Os-^{187}Os and highly siderophile element
342 abundance systematics of the mantle revealed by abyssal peridotites and Os-rich alloys.
343 Geochimica et Cosmochimica Acta 200, 232-254
344 Ding S, Hough, T, and Dasgupta R (2018) New high pressure experiments on sulfide saturation
345 of high-FeO* basalts with variable TiO2 contents – implications for the sulfur inventory of the
346 lunar interior. Geochimica et Cosmochimica Acta 222, 319-339
347 Frost DJ, and McCammon CA (2008) The redox state of Earth's mantle. Annual Reviews of
348 Earth and Planetary Sciences 36, 389-420
349 Gibson EK Jr, and Moore GW (1974) Sulfur abundances in the valley of Tauru-Littrow. Proc.
350 Lunar Sci. Conf. 5th, 1823-1837
351 Gibson EK Jr, Usselman TM, and Morris RV (1976) Sulfur in Apollo 17 basalts and their source
352 regions. Proc. Lunar. Sci. Conf. 7th, 1491-1505
353 Gibson EK Jr, Brett R, and Andrawes F (1977) Sulfur in lunar mare basalts as a function of bulk
354 composition. Proc. Lunar Sci. Conf. 8th, 1417-1428
355 Giguere T, Taylor GJ, Hawke BR, and Lucey PG (2000) The titanium contents of lunar mare
356 basalts. Meteoritics and Planetary Science 35, 193-200
357 Haggerty SE (1978) The redox state of planetary basalts. Geophysical Research Letters 5, 443-
358 446
359 Haughton DR, Roeder PL, and Skinner BJ (1974) Solubility of sulfur in mafic magmas.
360 Economic Geology 69, 451-462

361 Hauri EH, Weinreich T, Saal A, Rutherford M, and Van Orman JA (2011) High pre-eruptive
362 water contents preserved in lunar melt inclusions. Science 333, 213-215
363 Holzheid A, and Grove TL (2002) Sulfur saturation limits in silicate melts and their implications
364 for core formation scenarios for terrestrial planets. American Mineralogist 87, 227-237
365 Horan MF, Walker RJ, Morgan JW, Grossman JN, and Rubin A (2003) Highly siderophile
366 elements in chondrites. Chemical Geology 196, 5-20
367 Jacobson SA, Morbidelli A, Raymond SN, O'Brien DP, Walsh KJ, and Rubie DC (2014)
368 Highly siderophile elements in Earth's mantle as a clock for the Moon-forming impact. Nature
369 508, 84-87
370 Kruijer T, Kleine T, Fischer-Gödde M, and Sprung P (2015) Lunar tungsten isotopic evidence
371 for the late veneer. Nature 520, 534-537
372 Lodders K (2003) Solar System abundances and condensation temperatures of the elements.
373 Astrophysical Journal 591, 1220-1247
374 Lorand JP, and Luguet A (2016) Chalcophile and siderophile elements in mantle rocks: Trace
375 elements controlled by trace minerals. Reviews in Mineralogy and Geochemistry 81, 441-488
376 Mann U, Frost DJ, Rubie DC, Becker H, and Audétat A (2012) Partitioning of Ru, Rh, Pd, Re, Ir
377 and Pt between liquid metal and silicate at high pressures and temperatures – Implications for
378 the origin of highly siderophile element concentrations in the Earth's mantle. Geochim.
379 Cosmochim. Acta 84, 593-613
380 Mavrogenes JA, and O'Neill HStC (1999) The relative effects of pressure, temperature and
381 oxygen fugacity on the solubility of sulfide in mafic magmas. Geochimica et Cosmochimica
382 Acta 63, 1173-1180

383 McDonough WF, and Sun S-S (1995) The composition of the Earth. Chemical Geology, 120,
384 223-254
385 Meisel T, Walker RJ, Irving AJ, and Lorand J-P (2001) Osmium isotopic compositions of mantle
386 xenoliths: a global perspective. Geochimica et Cosmochimica Acta 65, 1311-1323
387 Mungall JE and Brennan JM (2014) Partitioning of platinum-group elements and Au between
388 sulfide liquid and basalt and the origins of mantle-crust fractionation of the chalcophile
389 elements. Geochimica et Cosmochimica Acta 125, 265-289
390 Neal CR, and Taylor LA (1992) Petrogenesis of mare basalts - a record of lunar volcanism.
391 Geochimica et Cosmochimica Acta 56, 2177-2211
392 Ni P, Zhang Y, and Guan Y (2017) Volatile loss during homogenization of lunar melt inclusions.
393 Earth and Planetary Science Letters 478, 214-224
394 O'Neill HSC (1991) The origin of the Moon and the early history of the Earth—A chemical
395 model. Part 2: The Earth. Geochimica et Cosmochimica Acta 51, 1159-1172
396 O'Neill HSC, and Mavrogenes JA (2001) The sulfide capacity and the sulfur content at sulfide
397 saturation of silicate melts at 1400 C and 1 bar. Journal of Petrology 43, 1049-1087
398 Paniello RC, Day JMD, and Moynier F (2012) Zinc isotopic evidence for the origin of the Moon.
399 Nature 490, 376-379
400 Rees CE, and Thode HG (1972) Sulphur concentrations and isotope ratios in lunar samples.
401 Proc. Lunar Sci. Conf. 3rd, 1479-1485
402 Rees CE, and Thode HG (1974) Sulfur concentrations and isotope ratios in Apollo 16 and 17
403 samples. Proc. Lunar Sci. Conf. 5th, 1963-1973
404 Reid AM, Meyer C, Harmon RS, and Brett R (1970) Metal grains in Apollo 12 igneous rocks.
405 Earth and Planetary Science Letters 9, 1-5

406 Sato M (1978) Oxygen fugacity of basaltic magmas and the role of gas-forming elements.
407 Geophysical Research Letters 5, 447-449
408 Sato M, Hickling NL, and McLane JE (1973) Oxygen fugacity values of Apollo 12, 14, and 15
409 lunar samples and reduced state of lunar magmas. Proceedings of the Fourth Lunar Science
410 Conference, 1061-1079
411 Schlichting HE, Warren PH, and Yin QZ (2012) The last stages of terrestrial planet formation:
412 dynamical friction and the late veneer. Astrophysical Journal 752, 8pp
413 Schreiber HD, Balazs GB, Shaffer AP, and Jamison PL (1982) Iron metal production in silicate
414 melts through the direct reduction of Fe (II) by Ti (III), Cr (II), and Eu (II). Geochimica et
415 Cosmochimica Acta 46, 1891-901
416 Snyder GA, Taylor LA, and Neal CR (1992) A chemical model for generating the sources of
417 mare basalts: Combined equilibrium and fractional crystallization of the lunar magmasphere.
418 Geochimica et Cosmochimica Acta 56, 3809-3823
419 Steenstra ES, Seegers AX, Eising J, Tomassen BG, Webers FP, Berndt J, Klemme S, Matveev S,
420 and van Westrenen W (2018) Evidence for a sulfur-undersaturated lunar interior from the
421 solubility of sulfur in lunar melts and sulfide-silicate partitioning of siderophile elements.
422 Geochimica et Cosmochimica Acta 231, 130-56
423 Taylor SR, and McLennan SM (1985) The Continental Crust: Its Composition and Evolution: An
424 Examination of the Geochemical Record Preserved in Sedimentary Rocks. Blackwell, Oxford,
425 UK
426 Taylor SR, Taylor GJ, and Taylor LA (2006) The Moon – a Taylor perspective. Geochimica et
427 Cosmochimica Acta 70, 5904-5918

428 Touboul M, Puchtel IS, and Walker RJ (2015) Tungsten isotopic evidence for disproportional
429 late accretion to the Earth and Moon. Nature, 520, 530-533
430 Wadhwa M (2008) Redox conditions on small bodies, the Moon and Mars. Reviews in
431 Mineralogy and Geochemistry 68, 493-510
432 Walker RJ, Horan MF, Shearer CK, and Papike JJ (2004) Low abundances of highly siderophile
433 elements in the lunar mantle: evidence for prolonged late accretion. Earth and Planetary
434 Science Letters 224, 399-413
435 Wang K, and Jacobsen SB (2016) Potassium isotopic evidence for a high-energy giant impact
436 origin of the Moon. Nature 538, 487-490
437 Warren PH, and Taylor GJ (2014) The Moon. In: Davis AM (Ed.) Treatise in Geochemistry,
438 Vol. 1. Elsevier, Amsterdam, Edition 2, pp. 213-250
439 Warren, PH, Jerde EA, and Kallemeyn GW (1989) Lunar meteorites: siderophile element
440 contents and implications for the composition and origin of the Moon. Earth and Planetary
441 Science Letters, 91, 245-260
442 Weber RC, Lin P-Y, Garnero EJ, Williams Q, and Lognonne P (2011) Seismic detection of the
443 lunar core. Science, 331, 309-312
444 Wing BA, and Farquhar J (2015). Sulfur isotope homogeneity of lunar mare basalts. Geochimica
445 et Cosmochimica Acta, 170, 266-280
446 Yamashita N, Hasebe N, Reedy RC, Kobayashi S, Karouji Y, Hareyama M, Shibamura E,
447 Kobayashi MN, Okudaira O, d'Uston C, and Gasnault O. (2010) Uranium on the Moon:
448 Global distribution and U/Th ratio. Geophysical Research Letters 37

This is a preprint, the final version is subject to change, of the American Mineralogist (MSA)
Cite as Authors (Year) Title. American Mineralogist, in press.
DOI: https://doi.org/10.2138/am-2018-6386

449 **Figures and figure captions**

450

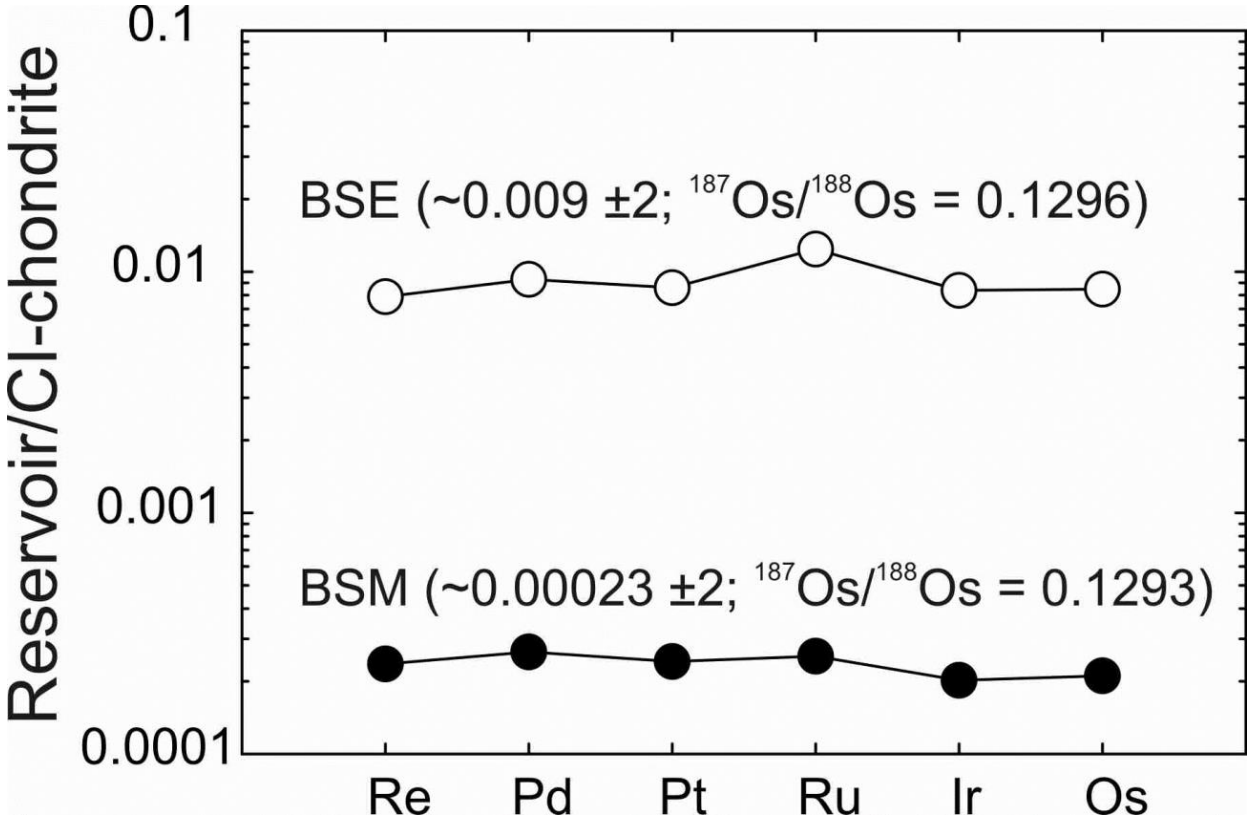

451

452

453 **Figure 1:** Estimated highly siderophile elements abundances in the bulk silicate Earth (BSE =
454 primitive mantle) and the bulk silicate Moon (BSM), normalized to Carbonaceous Ivuna (CI)
455 chondrite. BSE and BSM estimates are from Day et al. (2016), and CI-chondrite normalization is
456 from Horan et al. (2003). Here, BSE and BSM are considered to equate to mantle compositions,
457 since crustal reservoirs contain a relatively minor total fraction of the highly siderophile
458 elements.

This is a preprint, the final version is subject to change, of the American Mineralogist (MSA)
Cite as Authors (Year) Title. American Mineralogist, in press.
DOI: https://doi.org/10.2138/am-2018-6386

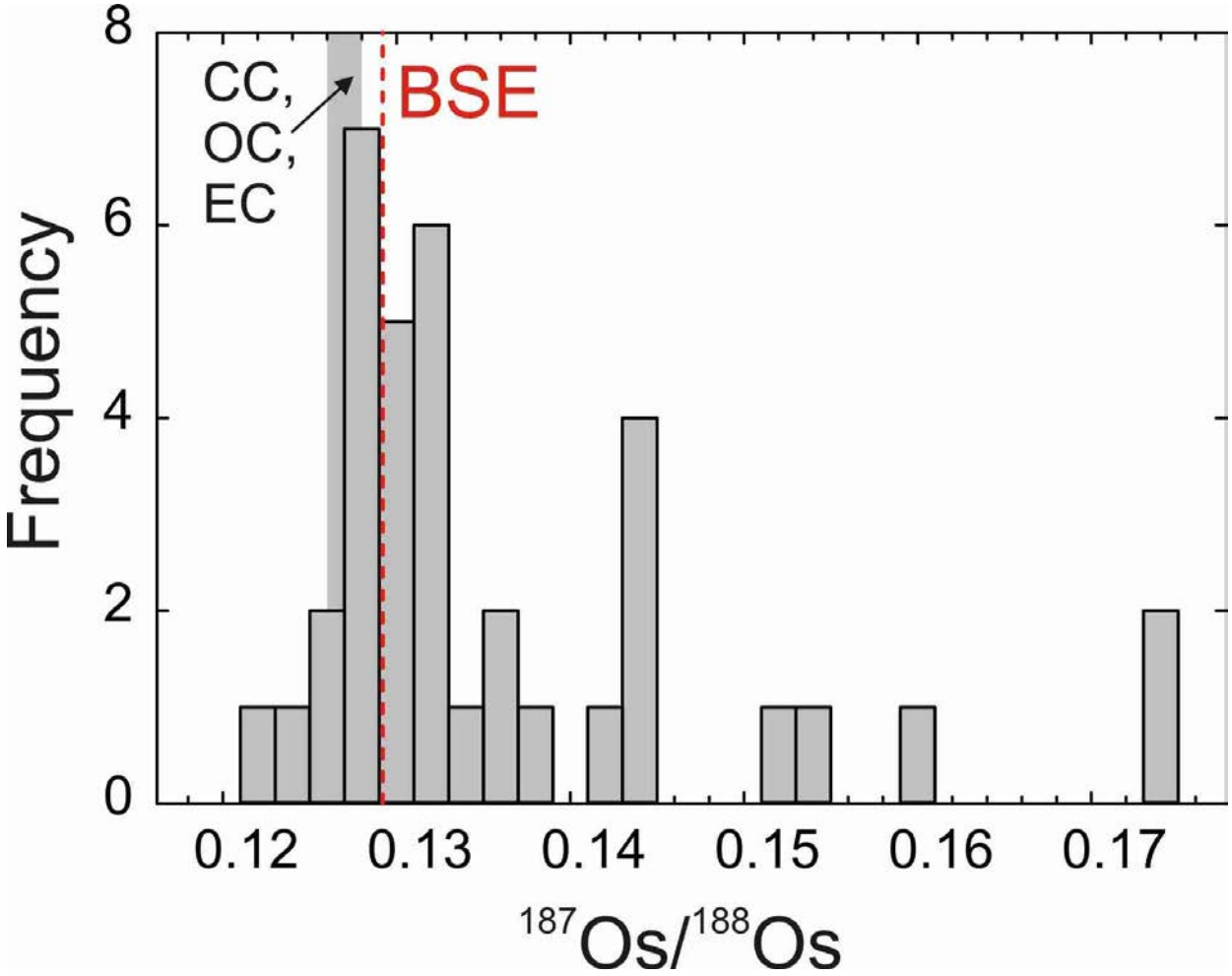

Figure 2: Histogram of measured $^{187}Os/^{188}Os$ ratios for lunar mare basalts from the Apollo 12, 15 and 17 sites versus the estimated bulk silicate Earth composition (red dashed line from Meisel et al., 2001; Day et al., 2017) and the typical range of carbonaceous, enstatite and ordinary chondrites (CC, EC, OC, shaded region from Day et al., 2016). Lunar mare basalt data are from Day et al. (2007) and Day & Walker (2015).

This is a preprint, the final version is subject to change, of the American Mineralogist (MSA)
Cite as Authors (Year) Title. American Mineralogist, in press.
DOI: https://doi.org/10.2138/am-2018-6386

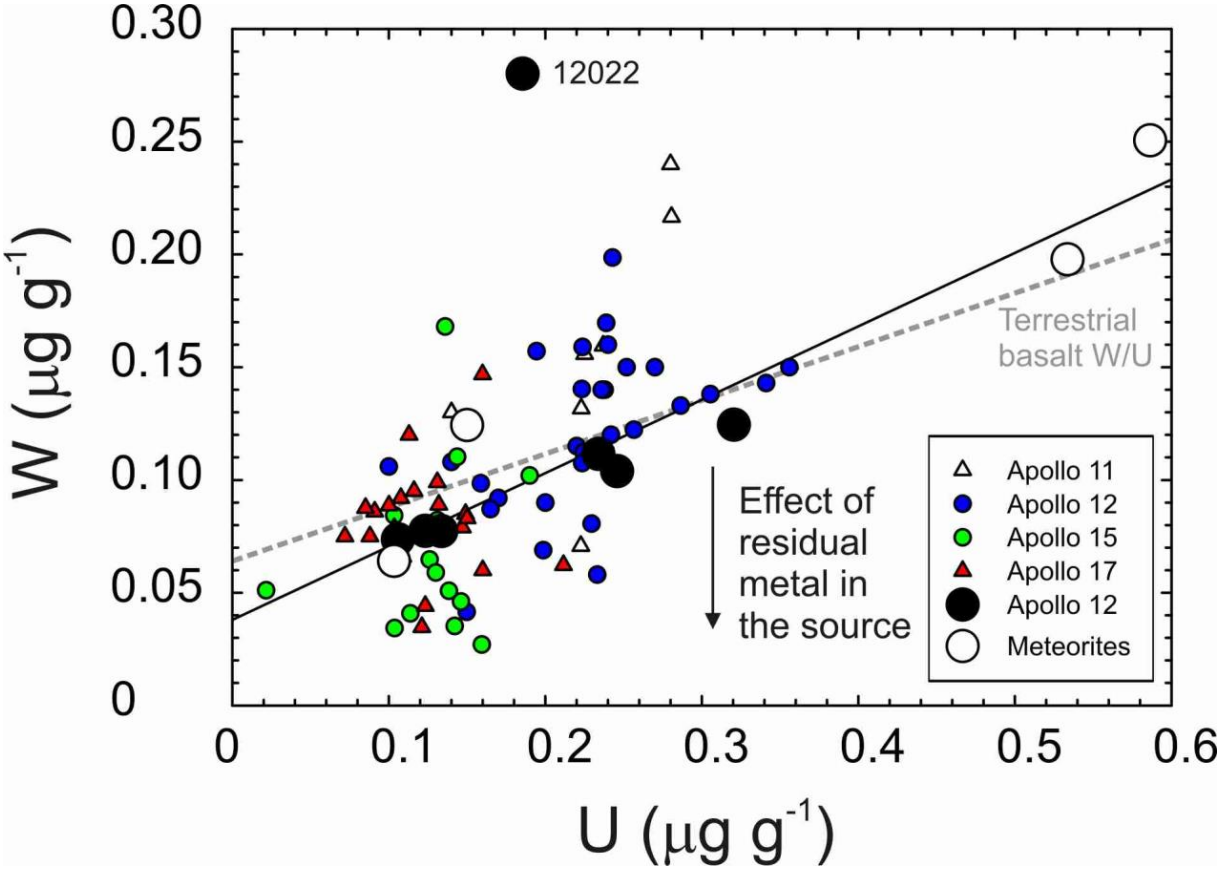

Figure 3: Uranium versus W concentrations in mare basalts from the Apollo 12 site (Day & Walker, 2015; filled circles), low-Ti mare basalt meteorites (Meteorites; unfilled circles) and published Apollo 11, 12, 15 and 17 mare basalt data (triangles for high-Ti Apollo 11 and 17, and small circles for low-Ti Apollo 12 and 15 samples). Apart from 12022 (0.28 µg g^{-1} W), the new Apollo 12 and low-Ti mare basalt data (large symbols) show linear correlations between W, U and Th and this dataset shows a positive correlation (solid line) with an r^2 of ~0.92, similar to W/U in terrestrial lavas. The high W content of 12022 is inconsistent with metal in the source, which would act to retain W. New data are presented in Table 1, together with a compendium of lunar mare basalt data compiled by C.R. Neal.

This is a preprint, the final version is subject to change, of the American Mineralogist (MSA)
Cite as Authors (Year) Title. American Mineralogist, in press.
DOI: https://doi.org/10.2138/am-2018-6386

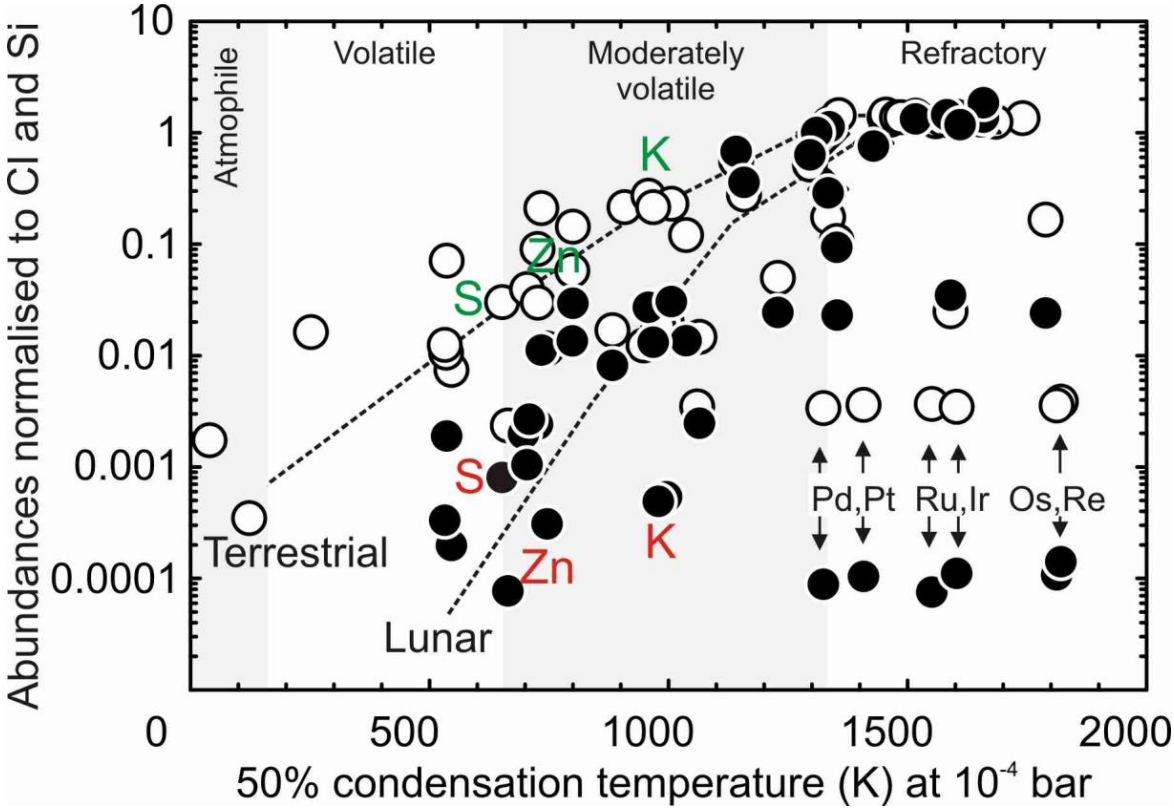

Figure 4: Estimated abundances of the elements classified according to their 50% condensation temperatures at 10^{-4} bar (from Lodders, 2003) in the mantles of Earth (unfilled circles) and the Moon (filled circles). Highlighted are the S, Zn and K abundances for Earth (green) and the Moon (red). Data are from O'Neill (1991), McDonough & Sun (1995), with highly siderophile element abundance data for the Moon from Day et al. (2007) and for Earth from Becker et al. (2006).

This is a preprint, the final version is subject to change, of the American Mineralogist (MSA)
Cite as Authors (Year) Title. American Mineralogist, in press.
DOI: https://doi.org/10.2138/am-2018-6386

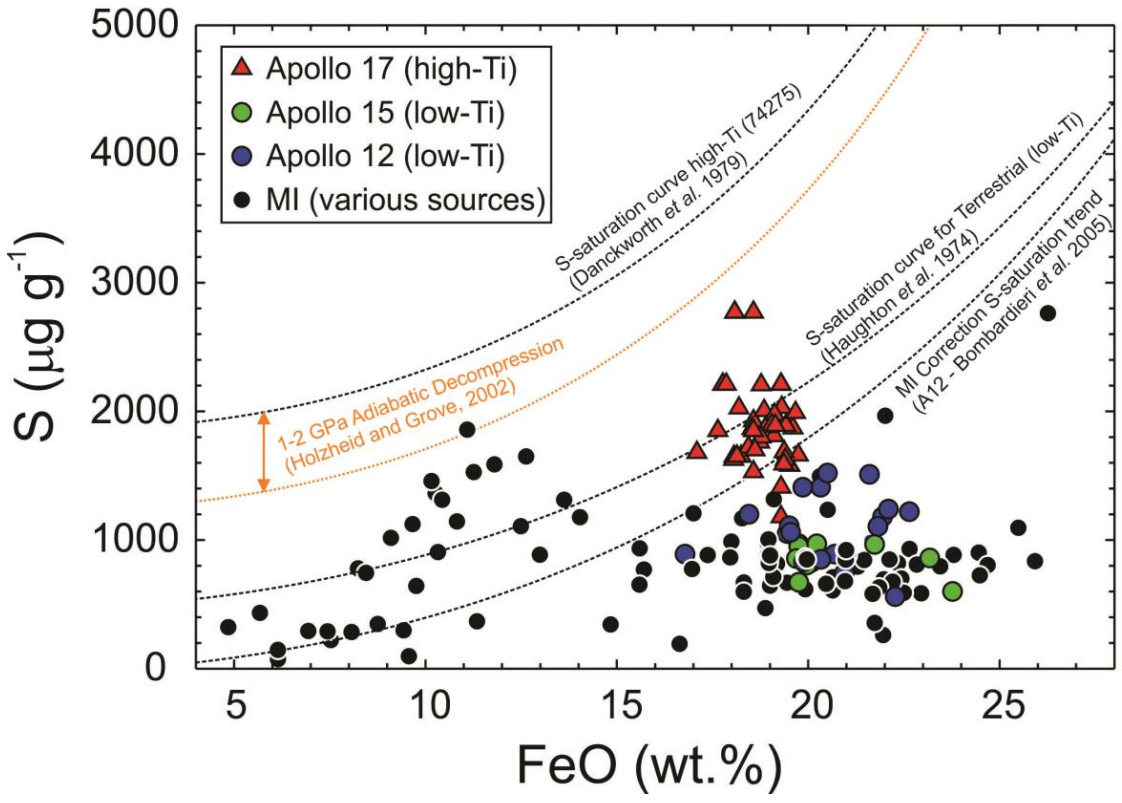

Figure 5: Contents of FeO versus S for mare basalt bulk rocks from the Apollo 12, 15 and 17 sites and for melt inclusions within olivine grains from Apollo 12 mare basalts and the lunar pyroclastic glass, 74220. Sulfur saturation curves are from Haughton et al. (1974), Danckworth et al. (1979), Holzheid & Grove (2002) and Bombardieri et al. (2005) with bulk rock data and melt inclusion data from Rees & Thode, (1972; 1974), Gibson & Moore (1974), Gibson et al. (1976; 1977), Bombardieri et al. (2005), Hauri et al. (2011), Chen et al. (2015), Ni et al. (2017). For reference, the S-saturation curve of high-Ti basalts from O'Neill & Mavrogenes (2002) at higher temperature is 0.4 units above the Danckwerth et al. (1979) curve.

This is a preprint, the final version is subject to change, of the American Mineralogist (MSA)
Cite as Authors (Year) Title. American Mineralogist, in press.
DOI: https://doi.org/10.2138/am-2018-6386

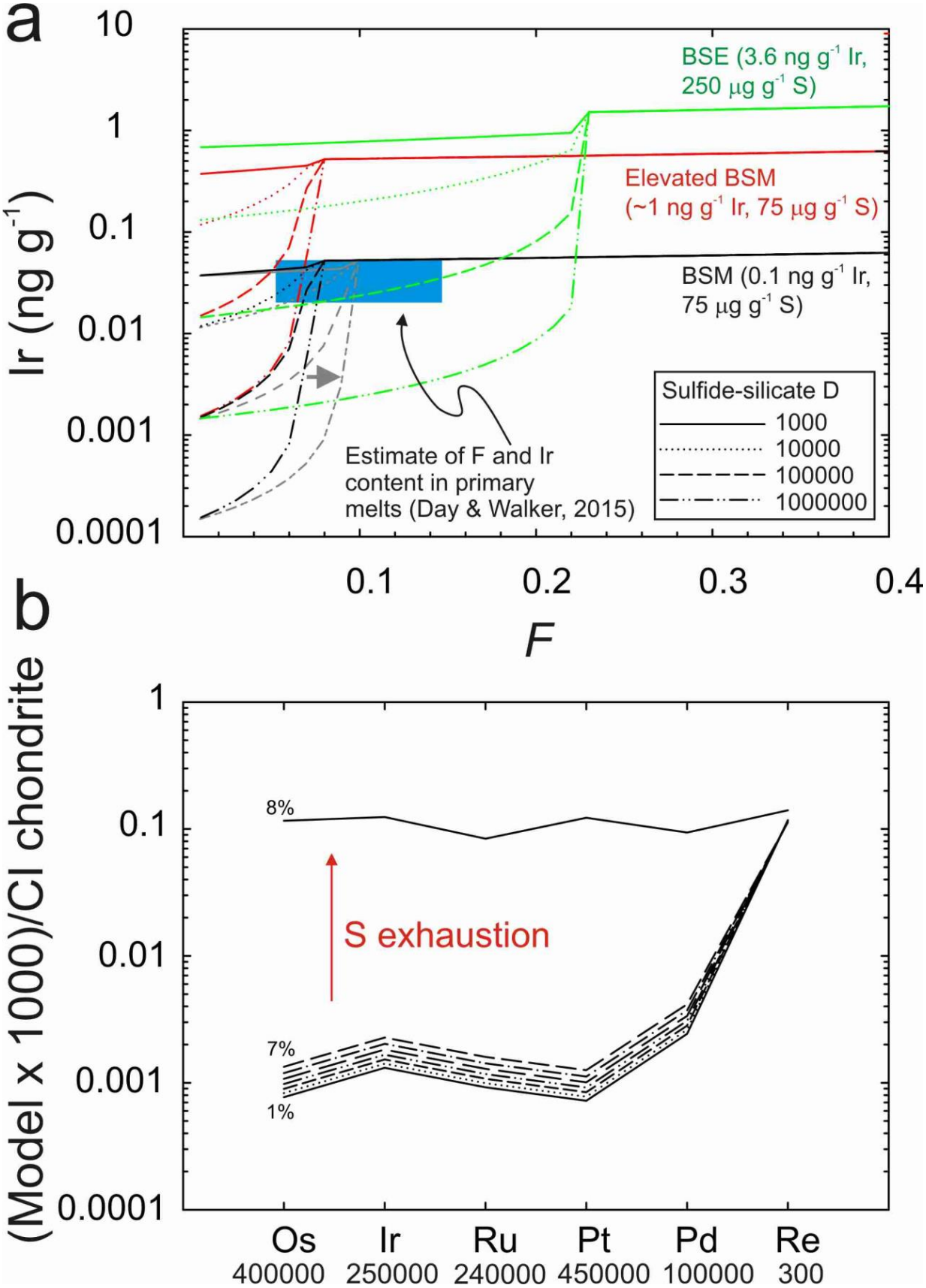

This is a preprint, the final version is subject to change, of the American Mineralogist (MSA)
Cite as Authors (Year) Title. American Mineralogist, in press.
DOI: https://doi.org/10.2138/am-2018-6386

Figure 6: Melting models for (a) Ir concentrations as a function of partial melting for different sulfide-melt partitioning (1000, 10,000, 100,000, 1,000,000; Mungall & Brenan, 2014) in a columnar melting regime, with three potential mantle sources, with 1050 μg g^{-1} S in the melt composition (Bombarderi et al., 2005) and lower estimates of SCSS for a BSM with low Ir content (~0.1 ng g^{-1}; grey model curves). The effect of lower SCSS is to drive exhaustion of the HSE during partial melting to the right (arrow). Models are for a terrestrial mantle source with BSE HSE abundances and 250 μg g^{-1} S (BSE Model); a lunar mantle source with BSM HSE abundances (e.g., Day et al., 2007; Day & Walker, 2015) and 75 μg g^{-1} S in the source (BSM Model); a source with ~25% of the BSE HSE estimate and 75 μg g^{-1} S in the source (Elevated BSM Model). For the models, the behavior of Ir in silicates is assumed to be relatively compatible (~1-2; Day, 2013). The grey shaded region shows the field for the highest HSE abundance Apollo 12 mare basalts and estimated degrees of partial melting to produce them from their source regions (Day & Walker, 2015). (b) Example of HSE inter-element fractionations that can arise for large and variable sulfide-melt partitioning. Sulfide-melt partitioning values are taken from Mungall & Brenan, 2014, anchoring values (shown beneath respective elements) to Pd sulfide-melt partitioning of 100,000. In this model (a lunar mantle source with BSM HSE abundances and 75 μg g^{-1} S in the source) S exhaustion occurs at ~8% partial melting and HSE patterns are distinctly non-chondritic.

This is a preprint, the final version is subject to change, of the American Mineralogist (MSA)
Cite as Authors (Year) Title. American Mineralogist, in press.
DOI: https://doi.org/10.2138/am-2018-6386

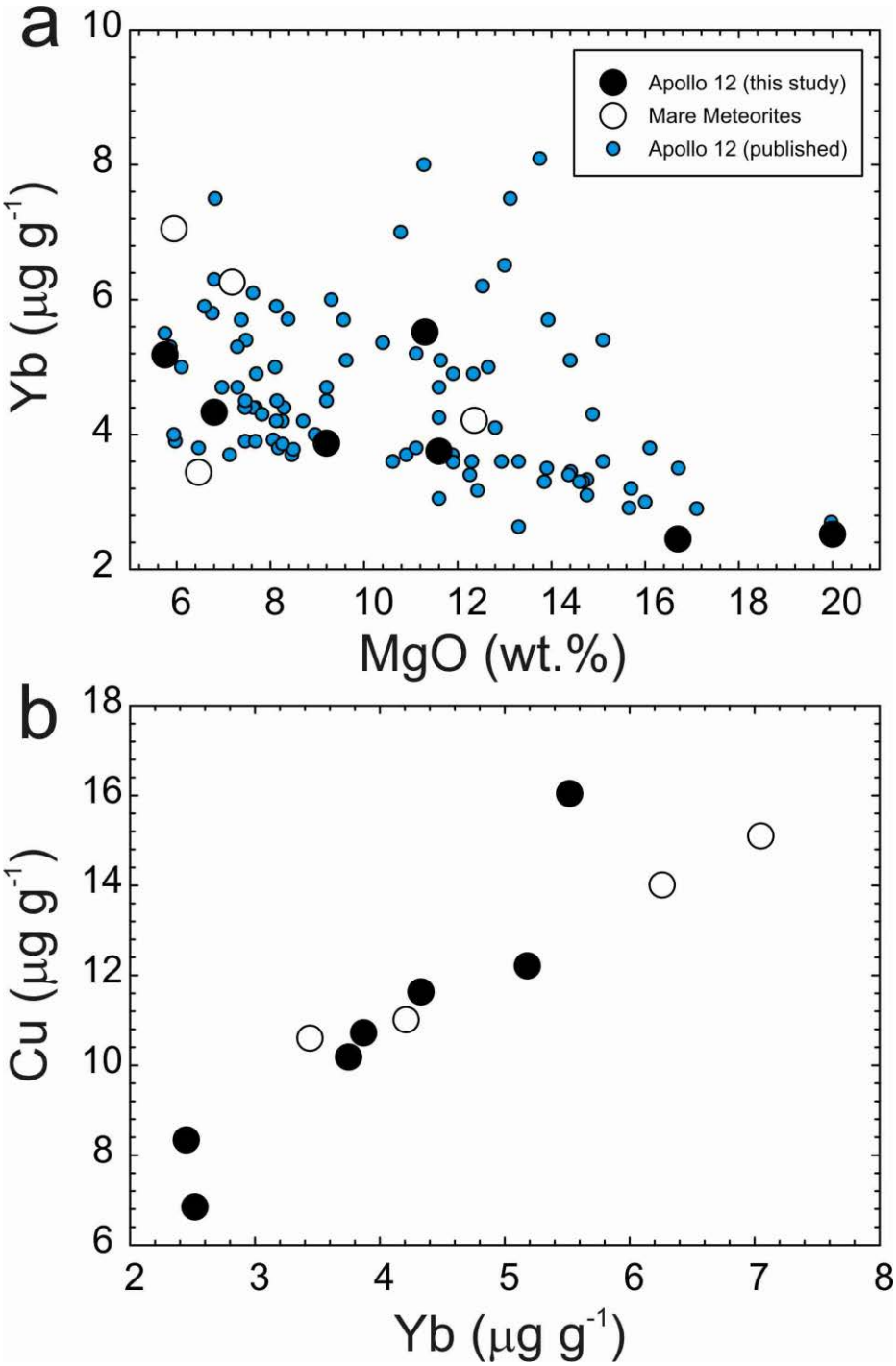

514

515 **Figure 7 -** (a) MgO versus Yb and (b) Yb versus Cu for Apollo 12 mare basalts and mare basalt
516 meteorites. Published data are from the compendium of mare basalt data compiled by C.R. Neal.

This is a preprint, the final version is subject to change, of the American Mineralogist (MSA)
Cite as Authors (Year) Title. American Mineralogist, in press.
DOI: https://doi.org/10.2138/am-2018-6386

Table 1: MgO, Yb, Th, U, W and Cu abundances for mare basalts

Sample	Type	MgO (wt.%)	Yb (µg g^{-1})	Th (µg g^{-1})	U (µg g^{-1})	W (ng g^{-1})	Cu (µg g^{-1})	U/Th	W/U
12009, 136	Olivine-norm	11.6	3.75	0.92	0.23	112	10.2	0.25	0.48
12040, 200	Olivine-norm	16.7	2.45	0.47	0.12	77	8.3	0.26	0.63
12039, 38	Pigeonite-norm	5.8	5.18	1.25	0.32	125	12.2	0.26	0.39
12019, 15	Pigeonite-norm	9.2	3.87	0.96	0.25	104	10.7	0.26	0.42
12022, 298	Ilmenite-norm	11.3	5.52	0.72	0.19	280	16.0	0.26	1.51
12005, 63	Ilmenite-norm	20.0	2.52	0.41	0.11	74	6.9	0.26	0.70
12038, 258	Feldspar-norm	6.8	4.33	0.57	0.13	77	11.6	0.24	0.58
MIL 05035	Low-Ti meteorite	6.5	3.44	0.47	0.10	64	10.6	0.22	0.62
LAP 02205	Low-Ti meteorite	5.9	7.05	2.42	0.59	251	15.1	0.24	0.43
NWA 4734	Low-Ti meteorite	7.2	6.26	2.06	0.53	198	14.0	0.26	0.37
Dho 287	Low-Ti meteorite	12.4	4.21	0.89	0.15	124	11.0	0.17	0.83
BHVO-2	(n = 6)	7.2	2.0	1.20	0.40	205	130.8	0.33	0.52
	RSD	3%	1%	3%	3%	9%	3%		

Fifty milligrams of sample powder, remaining after the determination of HSE abundances (Day et al., 2007; Day & Walker, 2015), were digested in HF/HNO_3 in teflon vials, dried down and sequentially taken up in HNO_3 to remove fluorides, and then doped with In and diluted to a factor of 1000 to analyze Yb, Th, U, W and Cu contents, and a factor of 10,000 to analyze MgO, using a Thermo Scientific iCAP Qc inductively coupled plasma mass spectrometer in normal mode at the Scripps Isotope Geochemistry Laboratory. Accuracy and precision were determined using terrestrial rock standards (BHVO-2, BCR-2, BIR-1, AGV-1) that were prepared from powders with samples. Some of the W concentrations were previously reported in Day & Walker (2015).